

Crystallization Kinetics of Linear Polyethylene at Elevated Pressures

Hsiung-To Tseng and Paul J. Phillips*†

Department of Materials Science and Engineering, University of Utah, Salt Lake City, Utah 84112. Received November 19, 1984

ABSTRACT: The crystallization behavior of linear polyethylene has been studied at pressures up to 2 kbar. Laser light scattering has been used to determine the pressure dependence of the regime I-regime II transition as well as the pressure dependence of spherulite growth rates in regime II. The regime I-regime II transition occurs at a constant supercooling and hence its location is determined by the pressure dependence of the equilibrium melting point. Analyses of linear growth kinetics using a secondary nucleation approach indicate the presence of pressure-independent fold surface free energy. Such an occurrence is believed to be consistent only with a tightly folded adjacent reentry critical nucleus. Studies of bulk kinetics detected the regime I-regime II transition, showing that it is important to the bulk crystallization of an unfractionated polymer and is not simply an effect associated with laboratory studies of sharp fractions.

Introduction

There have been many studies reported of the influence of crystallization pressure on the morphology of linear polyethylene.¹⁻⁷ These studies have concentrated on lamellar thickness variations and, in particular, the production of chain-extended crystals. Although the temperature and pressure conditions necessary for folded-chain and chain-extended crystallization have been determined carefully,⁷ there has been little attention paid to the rates of crystallization in either region.

In atmospheric-pressure crystallization, it is now well-established that at least two regions of crystallization exist.⁸⁻¹¹ Morphologically there is a change with increasing supercooling from axialites to spherulites in the region of 127 °C. This change is molecular weight dependent, being pronounced for lower narrow molecular weight fractions and nonexistent for molecular weights greater than 10⁵. There is a clear change in the rate of linear lamellar growth, leading to the designation of the phenomenon as a regime I-regime II transition related to the rate of deposition of secondary nuclei. So far, this transition has not been studied in unfractionated systems. Its dependence on crystallization pressure has not been considered; however, any transition should be pressure dependent.

Studies of the influence of crystallization pressure on the rate of lamellar growth and the lamellar thickness of *cis*-polyisoprene have been enlightening.¹²⁻¹⁵ It was recently shown that there is a large well-defined increase in the fold surface free energy with pressure.^{14,15} This effect is best explained in terms of a change in the conformational energy of the fold produced through a decrease in the effective volume of the fold, giving a large $P\Delta V$ effect which compensates for the increase in conformational energy associated with a more constricted structure. Clearly an analogous study of polyethylene would be valuable since a very tight adjacent reentry fold has generally been considered appropriate.⁹

In this contribution we report the results of an extensive experimental investigation into the bulk and linear growth rates of linear polyethylene as a function of pressure up to 2 kbar. The regime I-regime II transition has been seen in this unfractionated polymer in both bulk and linear growth experiments. Also the pressure dependence of the

fold surface free energy has been determined.

Experimental Section

Specimens. The polymer used was Sclair 2907 supplied by DuPont of Canada. It has M_n , M_w , M_z , and M_{z+1} values of 17 457, 61 000, 206 700, and 465 530, respectively. Thin sheets were prepared by using a hot press and chrome-plated steel plates and a melt temperature of 150 °C. Disks were punched from these films with steel punches of inner diameter 0.189 in. ground to a 30° angle at the tip.

Linear Growth Rate Studies. The most appropriate method for this study was laser light scattering.^{16,17} A Spectra Physics helium-neon laser Model 120S was used as the light source, and a Canon AE-1 camera was used to record the scattering patterns, all experiments being carried out with crossed polars. The high-pressure cell and generating system were essentially those already described by Dalal and Phillips¹⁴ with several modifications for high-temperature use. First, the specimen was placed between two sapphires in a precisely machined tube instead of Teflon shrink tubing, care being taken to ensure perfect alignment of the sapphires as discussed earlier.¹⁴ Seals were obtained by using silicone rubber O-rings backed by steel antiextrusion rings rather than fluorocarbon O-rings.¹⁴ Heating was achieved by using preheated silicone fluid circulated by a Haake thermostat bath in combination with three cartridge heaters to quickly reach the required temperature. The circulating liquid was held at a slightly lower temperature than required, the cartridge heaters being controlled by a Mettler FP5 control unit with the interfacing power amplifier described earlier.¹⁴ Both the constant temperatures required for crystallization experiments and the constant rates of heating required for melting point determinations could be achieved in this manner. The cell was first heated to a temperature of 20–30 °C above the melting point at pressure for 10–15 min in order to minimize any memory effects. The crystallization temperature was then applied as described above. During the isothermal crystallization process, the temperature was controlled by an RTD probe, a separate thermocouple being used to monitor the temperature. All premelting and crystallization experiments were carried out at pressure.

Melting Point and Light Transmission Studies. The high-pressure hot stage used here was the one described above, mounted on an optical microscope under crossed-polar conditions as described by Dalal and Phillips.¹⁴ Melting point experiments were as described by Dalal and Phillips¹⁴ whereas bulk crystallization studies involved continuous measurement and recording of the transmitted light intensity. The temperature lag in dynamic experiments between the sample and its heat exchanger was calibrated at atmospheric pressure and found to be linearly related to the scan rate. Since a similar calibration was impractical at elevated pressure, it was assumed that the thermal lag was pressure independent. Thermal conductivities generally increase with pressure but relatively slowly, and since the maximum pressure used was 2 kbar, any error would be small.

* To whom correspondence should be addressed at the Department of Materials Science and Engineering, University of Tennessee, Knoxville, TN 37996-2200.

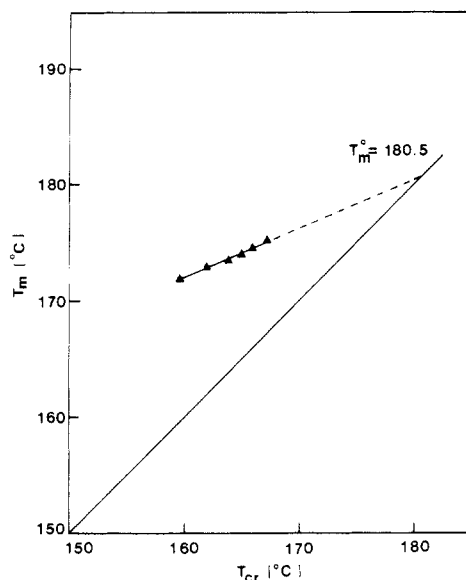


Figure 1. Plot of melting temperature vs. crystallization temperature for linear polyethylene (both crystallization and melting at 1.5 kbar).

Morphological and Thermal Studies. Specimens for microscopy and differential thermal analysis were crystallized, in a bomb in a compression mold. They were in the form of either premolded disks or thin films (50–300 μm thick), Teflon spacers being used to separate samples.

Differential scanning calorimetry was carried out at atmospheric pressure, as were X-ray diffraction experiments. Optical and electron microscopy studies were carried out on microtomed samples (30 μm thick). Permanganic etching¹⁸ was conducted by using 0.4% reagent and scanning electron microscopy was carried out. When necessary, carbon replicas were made of etched surfaces, which were then studied in a JEOL JEM200CX transmission electron microscope.

Results

Fusion Studies. The equilibrium melting points were estimated as a function of pressure using standard melting point vs. crystallization temperature plots (Figure 1). Results obtained (Figure 2) compare very well with those of Davidson and Wunderlich.¹⁹

Linear Growth Studies. Spherulites growing in regime II^{8–11} scatter light, producing cloverleaf patterns from which growth rates can be obtained by measuring the scattering angle giving rise to maximum intensity as a function of time. Axialites growing in regime I do not produce such patterns and hence the absence of a cloverleaf pattern can be taken as evidence of nonspherulitic growth. Carrying out a series of experiments as a function of crystallization temperature therefore leads to an estimation of the regime I–regime II transition temperature. Such studies have been carried out as a function of pressure and the transition temperatures plotted in Figure 3. The equilibrium melting point data are also plotted in Figure 3, where it can be seen that the pressure dependences of the regime I–regime II transition and the equilibrium melting point closely parallel one another. It seems, therefore, from this study that the regime I–regime II transition occurs at a constant supercooling and hence is determined by thermodynamic parameters. The transition observed here corresponds to the loss of a perfect cloverleaf scattering pattern and was not directly observed as in other studies.^{9,10} In fact, the transition was relatively broad in this case, taking approximately 1.5 $^{\circ}\text{C}$ for all vestiges of a cloverleaf to disappear. This effect is probably a result of the specimen being polydisperse, whereas those of other studies were sharp fractions. Since it is known

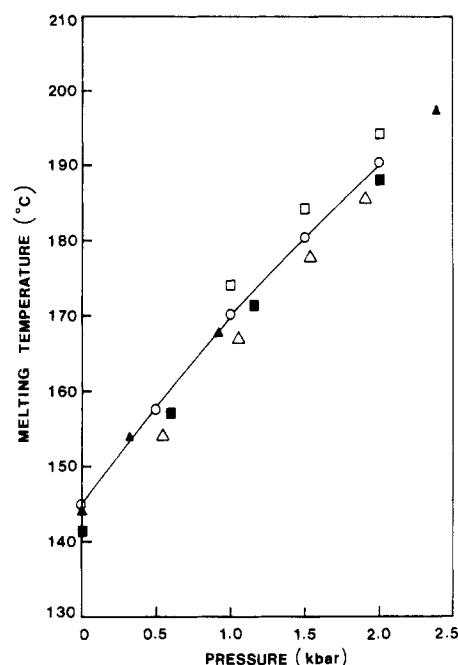


Figure 2. Equilibrium melting temperature vs. pressure: (○) this work; (□) Bassett and Turner⁵; (▲) Matsuoka³³; (■) Baer and Kardos³⁴; (Δ) Davidson and Wunderlich.¹⁹

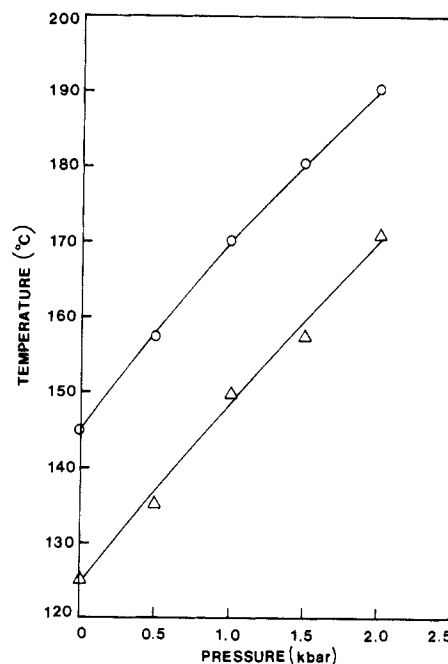


Figure 3. Melting point and regime I–regime II transition temperature as a function of pressure.

that the molecular weight has a strong effect on the existence of the transition as well as its manifestation, the use of a specimen of broad molecular weight would be expected to make the transition less well-defined.

For the estimation of linear growth rates, spherulite radii from light scattering were first compared with those obtained by direct measurement using optical microscopy. The radii from light scattering studies were slightly smaller than those from microscopy, in agreement with data of Stein and Rhodes.¹⁶ There was, however, a clear linear relation between the two measurements, preventing any question regarding the validity of growth rate data. All data obtained were linear up to impingement and showed no curvature at high conversions. Typical data for atmospheric-pressure crystallization are shown in Figure 4,

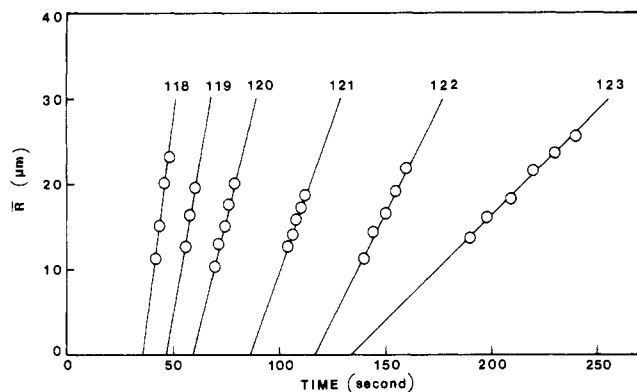


Figure 4. Atmospheric-pressure linear growth measurements from laser light scattering at the temperatures indicated.

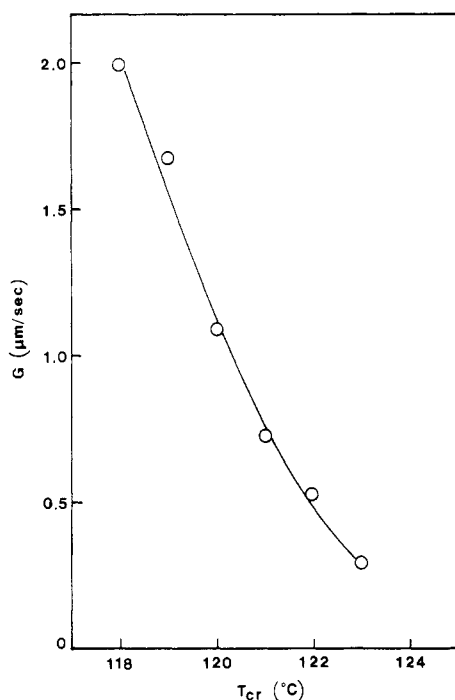


Figure 5. Linear growth rates at atmospheric pressure.

the linear growth rates obtained being shown in Figure 5 (all data being for the regime II region). Similar data at elevated pressures are shown in Figure 6. The data are all typical of the low supercooling side of a crystallization curve. The curves are displaced to higher temperatures at a rate of approximately 20 °C/kbar as would be expected for a polymer whose crystallization behavior is dominated by supercooling. In order to proceed further it is necessary to analyze the data by using secondary nucleation theory. Such a procedure will be detailed in the Discussion.

Bulk Growth Studies. The behavior of specimens was typical of the near-universal shape of curve first observed by Bekkedahl²⁰ for natural rubber. In each case there was a well-defined induction time during which no crystallization was observed by the detection system. After crystallization began, it proceeded at an accelerating rate followed by a decelerating stage and ultimately a pseudo-equilibrium transmitted light intensity resulted. This typical sigmoidal shape was obtained in each case with no sudden changes or discernible discontinuities. Initial analyses were carried out with half-time estimates, where $t_{1/2}$ is defined as the time for completion of 50% crystallization. In all cases the rate of crystallization was a strong function of crystallization temperature (Figure 7).

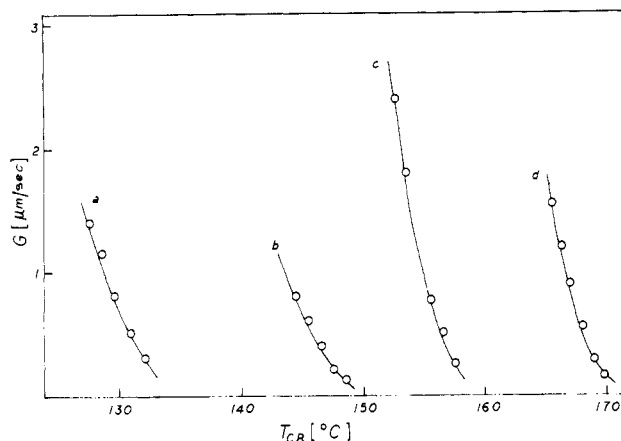


Figure 6. Linear growth rate dependence on pressure for (a) 0.5, (b) 1.0, (c) 1.5, and (d) 2.0 kbar.

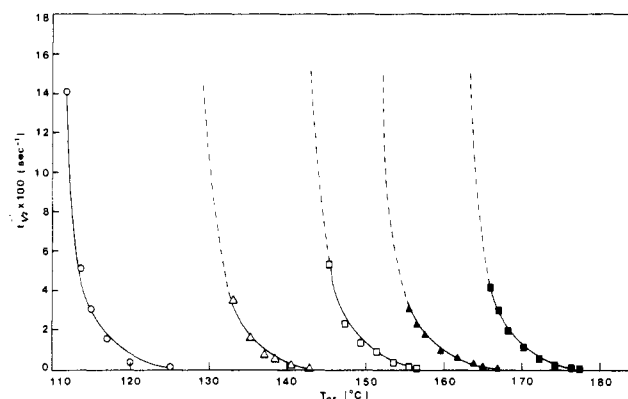


Figure 7. Reciprocal half-time of crystallization vs. temperature as a function of pressure: (○) atmospheric; (Δ) 0.5 kbar; (□) 1 kbar; (Δ) 1.5 kbar; (■) 2 kbar.

In contrast to the linear growth studies, however, data covered both regime I and regime II temperature ranges.

Discussion

First, let us consider the linear growth rate data typical of regime II or spherulite growth. A conventional plot of the Lauritzen-Hoffman formulation⁹ would be to use abscissa X and ordinate Y given by

$$X = 1/(T\Delta T)f \quad Y = \log G + U^*/[2.3R(T - T_\infty)]$$

the correction factor f being given by $f = 2T/(T_m^\circ + T)$.

It was decided to first process the atmospheric-pressure data using various parameters in order to assess the importance of variations. The equilibrium melting point of 144.5 °C is well established as is the value of the heat of fusion (ΔH_f) needed in the estimation of $\sigma\sigma_e$. Values of the unit cell parameters, a_0 and b_0 , are also known as a function of temperature.²¹ The major problem lies in the values of T_∞ and U^* to be used. Values used successfully in the past⁹ are $T_\infty \sim T_g - 30$, where $T_g = 231$ K and $U^* \approx 1500$ cal/mol. Recent analyses of Boyd²² produced a reliable value of T_g of 190 K whereas fluidity measurements²³ would suggest a value of $U^* \approx 4000$ cal/mol as more appropriate. In order to check the importance of these major variations the data were processed by using combinations of T_g 's of 190 and 231 with U^* values of 1500 and 3000 cal/mol. The results are presented in Figure 8, where it can be seen that all combinations given excellent fits with correlation coefficients higher than 99%. All the slopes produced closely similar values of K_g , which were converted by using

$$K_g(\text{II}) = 2b_0\sigma\sigma_e T_m^\circ / (\Delta H_f)k$$

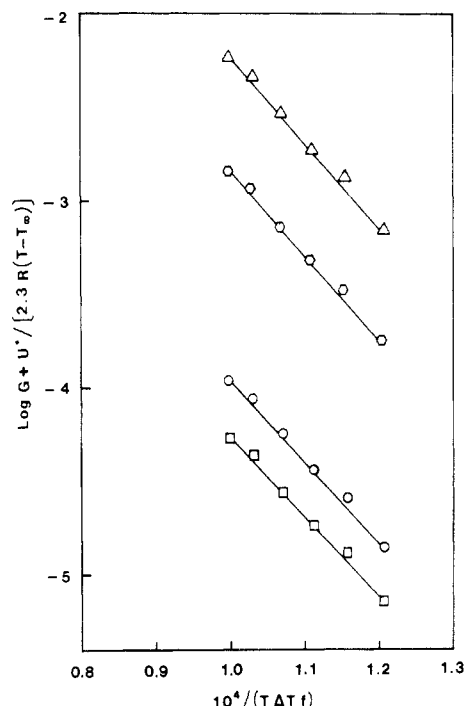


Figure 8. Analyses of linear growth kinetics at atmospheric pressure: (O) $U^* = 1500$ cal/mol, $T_\infty = 201$ K; (□) $U^* = 1500$ cal/mol, $T_\infty = 160$ K; (Δ) $U^* = 3000$ cal/mol, $T_\infty = 201$ K; (○) $U^* = 3000$ cal/mol, $T_\infty = 160$ K).

into values of $\sigma\sigma_e$, giving $1240 \text{ erg}^2/\text{cm}^4$. This value is quite close to the value of $1380 \text{ erg}^2/\text{cm}^4$ obtained by Hoffman et al.⁹ using optical microscopy.

In order to proceed to the analysis of high-pressure data, several assumptions need to be made. First, it was assumed that Lauritzen-Hoffman theory would be applicable, for the pressures considered, if all the parameters were corrected for the effect of pressure. Such a procedure was found to be effective for *cis*-polyisoprene.¹⁵

The variation in the dominant parameter, T_m° , with pressure was determined as part of this study and found to be in excellent agreement with data of Davidson and Wunderlich.¹⁹ The pressure dependence of the latent heat of fusion was not determined but was already known for pressures up to 1.6 kbar, having been determined by Karasz and Jones.²⁴ An extrapolation procedure was used to obtain a value for 2.0 kbar; however, this parameter is

Table I
Input Data of LPE for Linear Growth Rate Kinetic Analysis at Atmospheric Pressure

quantity	value	remarks
heat of fusion, ΔH_f	$2.8 \times 10^9 \text{ erg/cm}^3$	Hoffman et al. (1969)
equilibrium melting temperature, T_m°	144.5 °C	this work
glass transition temperature, T_g	231 °C	Hoffman et al. (1976)
activation energy, U^*	1500 cal/mol	Boyd (1984)
molecular width, a_0	$4.5426 \times 10^{-8} \text{ cm}$	Hoffman et al. (1976)
layer thickness, b_0	$4.1450 \times 10^{-8} \text{ cm}$	this work

Table II
Results of High-Pressure Kinetic Analysis of LPE from Linear Growth Rate Data

P , kbar	corr coeff, %	$K_g \times 10^{-5}$, K^2	$\sigma\sigma_e$, erg^2/cm^4	σ_e , erg/cm^2
0.001	99.65	1.1100	1240	87.94
0.5	99.70	1.2459	1335	94.64
1.0	99.78	1.2240	1266	89.83
1.5	99.94	1.2460	1214	86.10
2.0	99.25	1.3546	1342	95.18

relatively unimportant, being a weak function of pressure. Ito and Marui²⁵ studied the effects of pressure on the unit cell parameters. Their data were combined with thermal expansion data²¹ for our purposes. It was found that a_0 and b_0 had decreased by only 10% at 2.0 kbar.

We have not determined the variation of T_∞ and U^* with pressure, such a study being a major undertaking. For many polymers, values of dT_g/dP tend to be close to 20 °C/kbar. The above approximation combined with the relationship $T_\infty = T_g - 30$ has been used. U^* is not usually a strong function of pressure¹⁵ and so has been kept invariant. Since both T_∞ and U^* are not major variables in kinetic analyses of polyethylene, as demonstrated above, these assumptions should lead to a fairly reliable first approximation. All input data used are presented in Table I.

Plots of $\log G + U^*/[2.3R(T - T_\infty)]$ vs. $1/(T\Delta Tf)$ at 0.5, 1.0, 1.5, and 2.0 kbar are shown in Figure 9a-d. The 2.0-kbar data have been processed by using the various combinations of T_∞ and U^* and as can be seen, this produces little change in the fits as was observed for atmospheric-pressure data. All curves gave excellent fits with correlation coefficients greater than 99%. The products

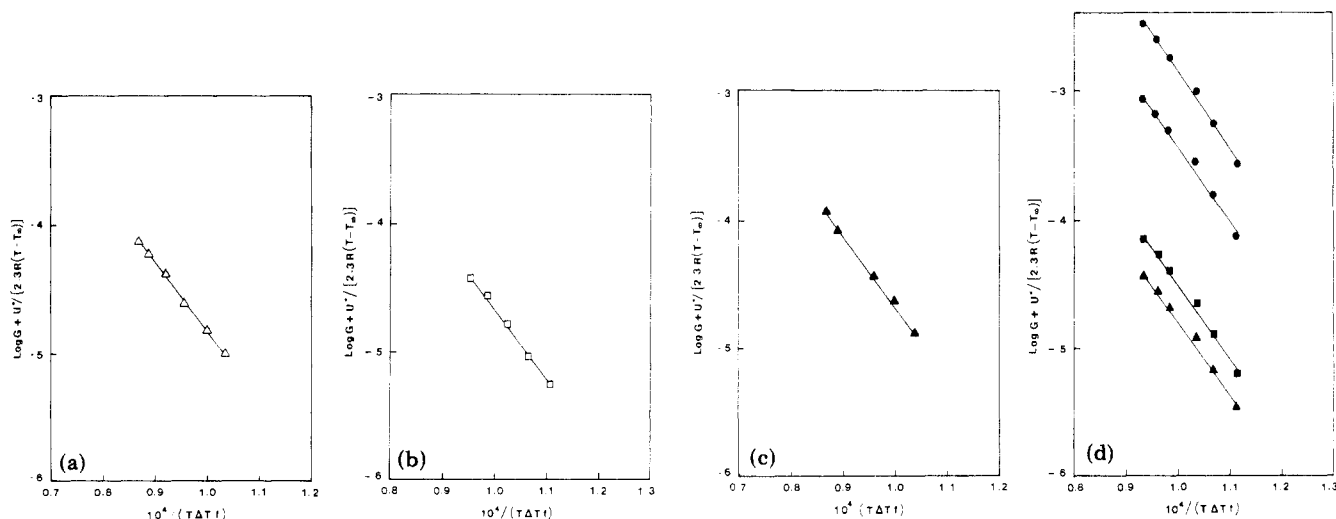


Figure 9. Linear growth rate analyses at elevated pressure: (a) 0.5 kbar; (b) 1.0 kbar; (c) 1.5 kbar; (d) 2.0 kbar [(■) $U^* = 1500$ cal/mol, $T_\infty = 241$ K; (Δ) $U^* = 1500$ cal/mol, $T_\infty = 200$ K; (○) $U^* = 3000$ cal/mol, $T_\infty = 241$ K; (●) $U^* = 3000$ cal/mol, $T_\infty = 200$ K].

of $\sigma\sigma_e$ obtained show slight deviations from atmospheric-pressure values (Table II); however, there is no consistency in the direction of the deviation. As expected, values of σ_e are relatively constant when calculated assuming a value of σ invariant at the atmospheric-pressure value of 14.1 erg/cm².

In contrast to studies of *cis*-polyisoprene,^{14,15} where a near doubling was observed over a narrow pressure range, the end surface free energy of the critical nucleus of polyethylene is independent of pressure. This is an important result which reflects a major difference in the conformational structure of the folds present in the two polymers. In the case of *cis*-polyisoprene, the behavior was explained in terms of a pressure-induced change in the fold conformation to a fold of lower volume which, being more cramped, would be of higher conformational energy. The gain from a $P\Delta V$ term would balance or exceed the increase in additional conformational energy. Initially such a fold would, of necessity, be relatively loose or conformational changes would be energetically prohibitive. Studies of Woodward et al.²⁶ using analyses of epoxidation reactions together with NMR experimentation have suggested as many as four monomer units for a fold in *cis*-polyisoprene. Studies using molecular models by Dalal and Phillips^{14,27} suggested that such a transition was possible in a fold containing as few as two monomer units (i.e., eight carbon-carbon bonds). In the case of polyethylene, the lack of a pressure dependence of fold surface energy suggests the presence of tight folds in which major conformational change is near impossible over the pressure range studied. Such a picture is, of course, consistent with the models of polyethylene folds that have been suggested for the past 20 or more years. The model of Frank and Tosi,²⁸ for instance, designed to produce the tightest possible fold, produces a conformation which would be difficult to contract without the incorporation of additional methylene units, thus increasing the volume of the fold. It has to be recognized that our analyses assume a temperature-independent fold surface free energy. Although the surface free energy must reflect changes in the nonadjacent reentry fraction, which should increase with increasing supercooling, the effects do not exceed the experimental error. An important point to be made, however, is that the end surface free energy obtained from crystallization kinetic analysis is that of the critical nucleus, which is composed of predominantly adjacent reentry folds.

Secondly, the bulk growth kinetics will be considered. There are two ways of handling such data and both should be considered. These are (a) half-time analyses and (b) Avrami analyses. The first method produces data of kinetic significance, the second of morphological relevance.

It was first shown by Magill²⁹ that there is a correspondence between half-time bulk data and linear growth rates. Bulk growth rate experimentation is much easier to carry out than linear growth rate studies. A major complication in bulk growth studies is the interference of secondary crystallization and ensuing difficulties in interpretation. Most studies have used techniques such as dilatometry which are susceptible to such effects. The use of transmitted light intensity under crossed-polar conditions tends to be unaffected by this problem, presumably because the transmitted light intensity is a result of scattering from anisotropic spheres. When the spheres have impinged, the light intensity remains constant. Analyses of such half-time data for branched and cross-linked polyethylenes using the Lauritzen-Hoffman approach were successful.³⁰ The analyses are very much dependent on the relative amounts of instantaneous and

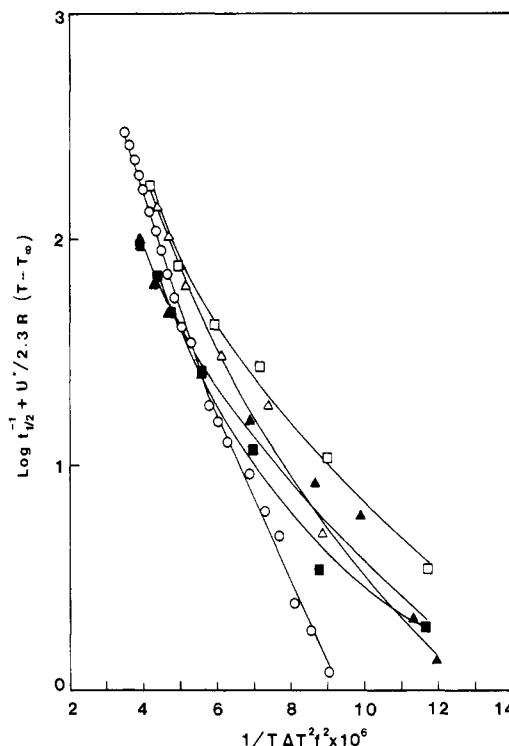


Figure 10. Ross-Frolen homogeneous nucleation analyses for bulk crystallization data at 1 bar (○), 0.5 kbar (△), 1.0 kbar (■), 1.5 kbar (▲), and 2 kbar (□).

sporadic nucleation present in the system. Ross and Frolen's analysis³¹ for homogeneous nucleation leads to a straight-line relation in a plot of $\log G + U^*/[2.3R(T - T_{\infty})]$ vs. $1/T(\Delta T)^2 f^2$. Substitution of G by $t_{1/2}^{-1}$ permits an estimation of the homogeneous or sporadic influence. Such plots for polyethylene at various pressures are shown in Figure 10, where it can be seen that except for atmospheric pressure, linear relationships are not present. Hence, crystallization processes at elevated pressures are not dominated by homogeneous nucleation and analyses of data can be attempted by using heterogeneous (or instantaneous) nucleation analyses. Under such circumstances, the bulk kinetic data will be a direct reflection of the linear growth processes.

The reason instantaneous (or heterogeneous) nucleation should be more important at elevated pressures is unknown. In *cis*-polyisoprene¹³ nucleation was always of a sporadic (or homogeneous) nature and indeed a peak in nucleation density was observed as a function of pressure at constant temperature, consistent with homogeneous primary nucleation theory. There were no obvious changes in spherulite size in these studies of polyethylene and so the effect cannot simply be explained in terms of one mechanism being enhanced by pressure; rather there appears to be a change in the time dependence of primary nucleation, with no major change in nucleation density occurring. Detailed histogrammic analyses of size distribution may cast further light on the problem but have not yet been carried out. In studies of branched and cross-linked polyethylenes³⁰ analyses using a straight substitution of $t_{1/2}^{-1}$ for G in the equations used earlier for linear growth rate analyses were found to produce values of $\sigma\sigma_e$ compatible with those from linear growth studies. Analyses have, therefore, been carried out with plots of $\log (1/t_{1/2}) + U^*/[2.3R(T - T_{\infty})]$ vs. $1/(T\Delta T f)$. Should this method be successful for linear polyethylene then it would permit studies to be carried out in temperature and pressure ranges inaccessible to the laser light scattering technique because of nonspherulitic morphologies.

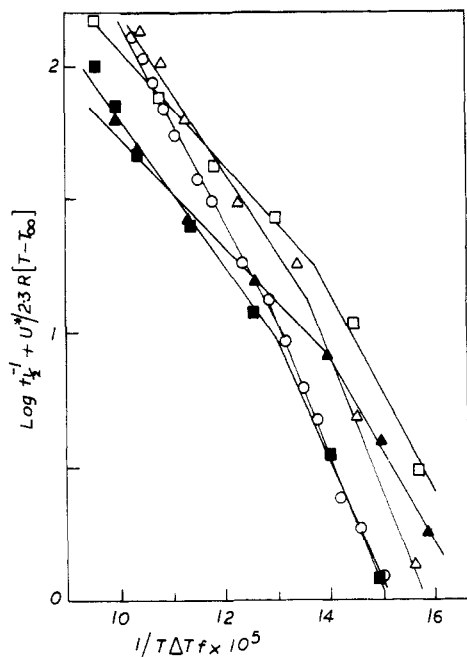


Figure 11. Half-time kinetic analyses assuming heterogeneous nucleation at (a) atmospheric pressure, (b) 0.5 kbar, (c) 1.0 kbar, (d) 1.5 kbar, and (e) 2.0 kbar (symbols as in Figure 7).

Table III
Results of the Half-Time Kinetic Analysis of LPE at Various Pressures

<i>P</i> , kbar	regime transition temp, °C	regime assumed	$\sigma\sigma_e$, erg ² /cm ⁴
0.001	125	I	652
	(125) ^a	II	933 (1240) ^a
0.5	139	I	630
	(136) ^a	II	729 (1335) ^a
1.0	152	I	445
	(150) ^a	II	533 (1266) ^a
1.5	163	I	393
	(158) ^a	II	483 (1214) ^a
2.0	173	I	525
	(170) ^a	II	525 (1342) ^a

^a Data in parentheses obtained from linear growth rate data.

Plots are shown in Figure 11, where it can be seen that a distinct break occurs at each pressure. For atmospheric pressure, the break point of 125 °C corresponds exactly to the regime I–regime II transition determined in the laser light scattering studies. For higher pressures, although the break is clearer, there is a discrepancy of 2–3 °C (Table III). An important point is, therefore, that the regime I–regime II transition can be detected in the bulk kinetics of an unfractionated polyethylene using this approach; it does not, however, coincide exactly with the axialite-spherulite transition. This observation is in itself a confirmation of the assumption that in a system in which heterogeneous nucleation dominates, conclusions regarding linear growth kinetics can be made from appropriately analyzed bulk kinetic data.

A more stringent test of the applicability of the procedure lies in the values of $\sigma\sigma_e$ obtained. Such data are also shown in Table III, where it can be seen that values obtained for both regime I and regime II differ significantly from the value obtained from linear growth rate data. The ratio of the values for regime II and regime I is also very different from the theoretical value of 2.0. It will be noted that the discrepancies are greatest for regime I, where the data may be influenced by the axialitic morphology not being composed of anisotropic spheres. The discrepancies

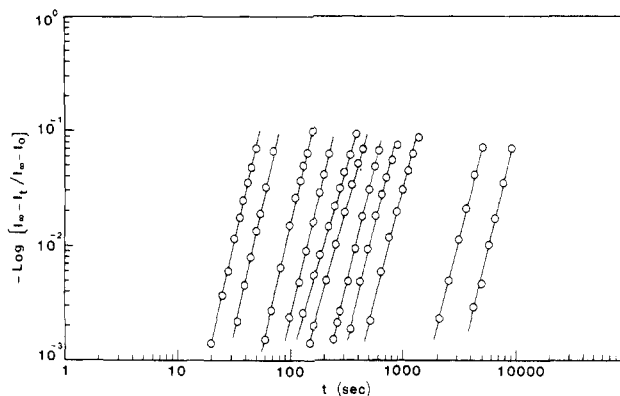


Figure 12. Avrami plots for atmospheric-pressure crystallization at temperatures of 118, 119, 121, 122, 123, 124, 125, 125.5, 126, 127.5, and 128 °C, respectively (left to right).

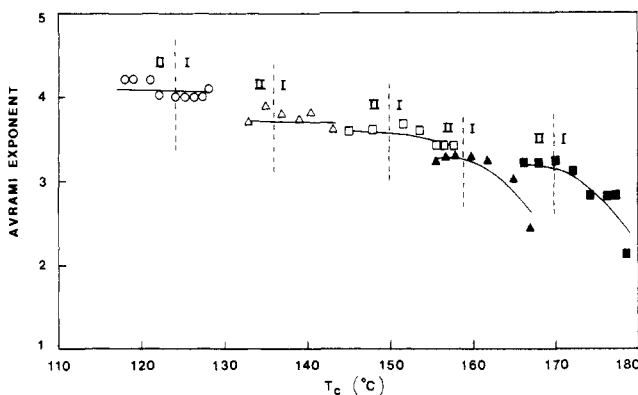


Figure 13. Avrami coefficients as a function of crystallization temperature at pressures of 1 bar (O), 0.5 kbar (Δ), 1.0 kbar (□), 1.5 kbar (▲), and 2.0 kbar (■).

are not likely to be due to the influence of nucleation processes on bulk crystallization. It can be observed from Figure 10 that each line has a different curvature, indicating different contributions from instantaneous and sporadic nucleation. Higher supercoolings generally favor sporadic nucleation and this effect may be responsible for the discrepancy at any particular pressure. The level of discrepancy is, however, strongly dependent on pressure, increasing with increasing pressure. Presumably, therefore, the nucleation process is changing significantly with pressure. However, it can be seen that there is a correlation between linear and bulk data and certain conclusions relevant to linear growth can be drawn from bulk data. In the case of the branched and cross-linked polyethylenes studies earlier,³⁰ nucleation was known to be predominantly instantaneous³² and better correlations in $\sigma\sigma_e$ were possible because of it.

Avrami analysis can be applied to transmitted light intensity data through the use of the plot³⁰ $\log \{-\log [(I_{\infty} - I_t)/(I_{\infty} - I_0)]\}$ vs. $\log t$. Typical curves are shown in Figure 12 for atmospheric-pressure crystallization at various supercoolings. The Avrami exponents were obtained as the slopes of fitted lines and are plotted in Figure 13 as a function of crystallization temperature for the different pressures used. It is clear that the values for the regime II region vary from close to 4 at atmospheric pressure to about 3 at 2 kbar, there being a progressive reduction as pressure is increased. The regime I region tends to have slightly lower values of the Avrami exponent except for pressures of 1.5 and 2 kbar, where they change from 3 to 2 over a short range of supercooling.

Morphological studies show the regime II spherulites to be of the banded morphological type throughout, in

agreement with Avrami exponent values. Conventional interpretations would ascribe the change in Avrami exponent from 4 to 3 as reflecting a change in nucleation patterns from sporadic to instantaneous. Such an observation is consistent with earlier comments on $t_{1/2}$ analyses which suggested a greater sporadic component at atmospheric pressure. In the axialitic region, detailed interpretation is difficult at this time. A change from 3 to 2 using theoretical models could be interpreted as a change from sporadic disk to instantaneous disk morphologies or a change from instantaneous sphere to instantaneous disk. The disk models might seem more appropriate for axialites; however, the situation is complicated because of the molecular weight distribution and the likely crystallization of the higher molecular weight fractions as regime II at all temperatures. Resolution of this problem must await detailed morphological evaluation together with studies on sharp fractions.

Conclusions

Pressure dependence of the fold surface free energy of the critical nucleus of polyethylene is consistent with the tightly folded adjacent reentry model over the range of pressures studied. Bulk kinetic studies can detect the presence of regime transitions when analyzed by a Lauritzen-Hoffman approach if the mode of nucleation is predominantly instantaneous in nature. Estimation of fold surface free energies using bulk kinetic data depends very much on the nucleation characteristics of the specimen being studied.

Acknowledgment. This research has been supported by the National Science Foundation, Polymers Program, under Grants DMR-8320212 and DMR-8106033.

Registry No. Sclair 2907, 9002-88-4.

References and Notes

- (1) B. Wunderlich and T. Arakawa, *J. Polym. Sci., Part A*, **2**, 3697 (1964).
- (2) B. Wunderlich and L. Melillo, *Makromol. Chem.*, **118**, 250 (1968).
- (3) R. B. Prime and B. Wunderlich, *J. Polym. Sci., Part A-2*, **7**, 2061 (1969).
- (4) D. V. Rees and D. C. Bassett, *J. Polym. Sci., Part A-2*, **9**, 385 (1971).
- (5) D. C. Bassett and B. Turner, *Nature (London), Phys. Sci.*, **240**, 146 (1972).
- (6) D. C. Bassett, S. Block, and G. J. Piermarini, *J. Appl. Phys.*, **45**, 4146 (1974).
- (7) D. C. Bassett, *Polymer*, **17**, 460 (1976).
- (8) J. I. Lauritzen and J. D. Hoffman, *J. Appl. Phys.*, **44**, 4340 (1973).
- (9) J. D. Hoffman, G. T. Davis, and J. I. Lauritzen, *Treatise Solid State Chem.*, **3** (1976).
- (10) J. Maxfield and L. Mandelkern, *Macromolecules*, **10**, 1141 (1977).
- (11) I. G. Voigt-Martin, E. W. Fischer, and L. Mandelkern, *J. Polym. Sci., Polym. Phys. Ed.*, **18**, 2347 (1980).
- (12) P. J. Phillips and B. C. Edwards, *J. Polym. Sci., Polym. Phys. Ed.*, **13**, 1819 (1975).
- (13) B. C. Edwards and P. J. Phillips, *J. Polym. Sci., Polym. Phys. Ed.*, **13**, 2117 (1975).
- (14) E. N. Dalal and P. J. Phillips, *Macromolecules*, **16**, 1754 (1983).
- (15) E. N. Dalal and P. J. Phillips, *Macromolecules*, **17**, 248 (1984).
- (16) R. S. Stein and M. B. Rhodes, *J. Appl. Phys.*, **31**, 1873 (1960).
- (17) R. van Antwerpen, Ph.D. Thesis, Delft, The Netherlands, 1971.
- (18) K. L. Naylor and P. J. Phillips, *J. Polym. Sci., Polym. Phys. Ed.*, **21**, 2011 (1983).
- (19) T. Davidson and B. Wunderlich, *J. Polym. Sci., Part A-2*, **7**, 377 (1969).
- (20) N. Bekkedahl, *Trans. Faraday Soc.*, **35**, 483 (1939).
- (21) S. Kavesh and J. M. Schultz, *J. Polym. Sci., Part A-2*, **8**, 243 (1970).
- (22) R. H. Boyd, *Macromolecules*, **17**, 903 (1984).
- (23) J. D. Ferry, "Viscoelastic Properties of Polymers", 2nd ed., Wiley, New York, 1970.
- (24) F. E. Karasz and L. D. Jones, *J. Phys. Chem.*, **71**, 2234 (1967).
- (25) T. Ito and H. Marui, *Polym. J.*, **2**, 768 (1971).
- (26) A. E. Woodward, personal communication.
- (27) E. N. Dalal, Ph.D. Thesis, University of Utah, 1983.
- (28) F. C. Frank and M. Tosi, *Proc. R. Soc. London, Ser. A*, **263**, 323 (1961).
- (29) J. H. Magill, *Nature (London)*, **187**, 770 (1960).
- (30) P. J. Phillips and Y. H. Kao, submitted for publication.
- (31) G. S. Ross and L. J. Frolen, *J. Res. Natl. Bur. Stand, Sect. A*, **79A**, 701 (1975).
- (32) R. M. Gohil and P. J. Phillips, submitted for publication.
- (33) S. Matsuoka, *J. Polym. Sci.*, **57**, 569 (1962).
- (34) E. Baer and J. L. Kardos, *J. Polym. Sci., Part A*, **3**, 2827 (1965).

Brillouin and Raman Scattering Studies of Single-Crystal-Texture Polyethylene

Paul J. Phillips*† and Y. T. Jang

Department of Materials Science and Engineering, University of Utah, Salt Lake City, Utah 84112

Q. L. Liu and Chin-Hsien Wang

Department of Chemistry, University of Utah, Salt Lake City, Utah 84112

John F. Rabolt

IBM Research Laboratory, San Jose, California 95193. Received August 24, 1984

ABSTRACT: Single-crystal-texture polyethylene has been made from linear low-density polyethylene by solid-state extrusion followed by high-pressure annealing. X-ray studies show the material to have the following orientation functions: $f_c(200) = 0.983$, $f_c(020) = 0.976$, and $f_c(002) = 0.989$. The material is semicrystalline with a sheet structure. Raman studies show the lamellar thickness to be distributed about a 92-Å maximum. Brillouin scattering studies confirm the single-crystal texture of the material. Longitudinal and transverse modes could be studied with both high precision and polarization discrimination for the first time.

Introduction

It is well-known that orientation can be produced in crystalline polymers through mechanical deformation.

* Present address: Department of Materials Science and Engineering, University of Tennessee, Knoxville, TN 37996-2200.

Although uniaxially oriented materials have been studied thoroughly, biaxially oriented polymers, normally produced by drawing and rolling,^{1,2} have received less attention. A special technique involving solid-state extrusion followed by high-pressure annealing was developed by Young and Bowden.³ When this technique was applied to linear